Available online at www.sciencedirect.com
SCIENCE DIRECT®
Mechanism and Machine Theory 41 (2006) 145–169
Mechanism and Machine Theory
www.elsevier.com/locate/mechmt

Kinematics, singularity and workspace of planar 5R symmetrical parallel mechanisms

Xin-Jun Liu [a,*], Jinsong Wang [a], G. Pritschow [b]

[a] *Manufacturing Engineering Institute, Department of Precision Instruments, Tsinghua University, Beijing 100084, PR China*

[b] *Institut für Steuerungstechnik (ISW), University of Stuttgart, Seidenstr. 36, D-70174, Stuttgart, Germany*

Received 16 November 2004; received in revised form 18 April 2005; accepted 10 May 2005
Available online 27 June 2005

Abstract

This paper treats the problems of kinematics, singularity and workspace analysis of the 5R symmetrical parallel mechanism. In the design process, the theoretical workspace cannot be used directly due to the inside singularity. The inverse and forward kinematic solutions determine the working and assembly modes of a mechanism. With different modes, a mechanism will have different singular loci and workspaces. In this paper, the singularity and usable workspace without singularity inside will be determined for the mechanism with a specified mode. A concept, the maximal inscribed workspace (MIW) that is bounded by the maximal inscribed circle (MIC), is defined to characterize the workspace performance. A non-dimensional design space is established to investigate the singular loci and workspace shape of the mechanisms, systematically. The atlas of the MIC radius is presented. Based on the obtained distribution charts of the singularity and workspace shape and the atlas, one can know the singularity and workspace performances of any one of the 5R symmetrical parallel mechanisms. The result, especially that of the MIW, of this paper is very useful for the optimum design of the mechanism.

Keywords: Parallel mechanism; Optimum design; Performance atlas; Workspace; Singularity

* Corresponding author.
E-mail address: xinjunl@yahoo.com (X.-J. Liu).

0094-114X/$ - see front matter © 2005 Elsevier Ltd. All rights reserved.
doi:10.1016/j.mechmachtheory.2005.05.004

1. Introduction

Analysis and optimum design are two important issues in the development of a parallel mechanism. Without exhaustive analysis, a design will not be perfect or even will be lost. Then, analysis is primary. In the design process, kinematics and workspace are two typical problems since they are the basic model and reference to define and evaluate the performances of a mechanism. For such a reason, the kinematics and workspace are the most studied issues in the field [1–6]. The efforts were motivated by the fact that they would be finally applied to the design and application of the devices. Two issues are involved in the optimal design of the mechanism: performance evaluation and dimensional synthesis. Having designed a mechanism, it is necessary to evaluate its performances. A second problem is to determine the dimensions (link lengths) of the mechanism, which is suitable for the task at hand. The latter one is one of the most difficult issues in this field. In the optimum design process, several performance criteria could be involved for a design purpose, such as workspace [7–9], singularity [9], dexterity [10,11], accuracy [12], stiffness [13], and conditioning index [9].

The five-bar mechanism is such a typical parallel mechanism with the minimal degrees of freedom (DoFs) in the field, which can be used for positioning a point on a region of a plane that is known as the workspace. The 5R parallel mechanism consists of five bars that are connected end to end by five revolute joints, two of which that are connected to the base are actuated. Such a mechanism with a symmetric structure attracted many researchers, who have investigated its position analysis [14], workspace [15,16], assembly modes [16,17], singularity [18,19], performance atlases [17,20] and kinematic design [19,21]. What is more, the symmetrical mechanism has been applied in the development of the MELFA RP Series robots in the Mitsubishi Electric Corporation.

The workspace of the mechanism has been studied using different methods [15,16,20], e.g., geometric and numerical approaches, including a novel, simple and powerful method for numerically generating the workspace developed in [16]. But most of them are related to the theoretical workspace, which is the region consisting of inside singularity. The singularity, especially the forward singularity, is the critical configuration that results in the change of working or assembly mode. Then, the singularity limits and separates the workspace of a mechanism. Once a mechanism is assembled with a specified mode, its workspace is determined. The mechanism must not access a singularity from one region to another. Although a workspace of the mechanism with a specified forward configuration (the *up-configuration*) was presented in [16], that was not enough to be applied in the practical design due to the singularity inside the workspace. A practical workspace is such a region without any singularity, in which the mechanism should be controllable. As well known, all global performance indices should be defined with respect to a workspace. In order to make the design more reasonable, it is necessary to present a workspace without singularity that can be used in the performance evaluation.

Although the singularity issue, especially singular loci, has been studied by other researchers [16,18,19], they have not been applied to the design of a 5R symmetric parallel mechanism yet. The reason for this is that they just showed the singularity in a general form. For example, all singular loci of the mechanism were illustrated in a developed chart in [19]. But, as we know, not all such singularities can occur for an assembled mechanism in practice. As the mechanism must not change its working or assembly mode from one to another, it is necessary to identify which singular loci the mechanism can have for a specified working or assembly mode.

According to the singularity classification by Gosselin and Angeles [4], the first kind of singularity (referred to as the *stationary singularity* in this paper) occurs when any one of the legs reaches its limit. The second kind of singularity (referred to as the *uncertainty singularity* in this paper) arises when the mechanism gains additional DoF(s). The first kind of singular locus is actually the theoretical workspace boundary. The second kind of singular locus is usually inside the workspace. Normally, there are tangent points between the two kinds of singular loci. At these points, the mechanism is actually in the configurations that change the working modes. The fact can be used to identify which singular locus a mechanism with a specified working mode can have. The result will help us to define a useful workspace. In this paper, the workspace without singularity inside is defined as the *usable workspace*, which is closer to the practical workspace than the theoretical workspace. As well known, a narrow usable workspace even with large area may be useless in practice as most points in such a workspace are near to the singularity. On contrary, a flat usable workspace even with smaller area could be of usefulness. For the purpose of decreasing the volume/workspace ratio of a device, the flattest part of the usable workspace is usually our research object. Such a workspace region always contains of most points far away from the singularity. Namely, this region has good control accuracy. Then, it is necessary to define an index to evaluate the flatness of a usable workspace. In this paper, the index is the radius of the MIC. The MIC is always in the flattest part of the usable workspace and is tangent with singular loci. The index is so useful that can characterize the workspace performance of the studied mechanism since a large MIC radius always leads to a large practical workspace. The maximal inscribed workspace (MIW) bounded by the maximal inscribed circle (MIC) can then be the region to define a global index evaluating a performance globally.

In this paper, in order to study all possible 5R parallel mechanisms, a design space is established according to the concept in [15,17,20]. In this paper, the design space is used to investigate the singularity and workspace systematically. The corresponding distribution charts for singular loci and usable workspace shape are obtained. From the charts, one can know how the singularity and usable workspace shape can be for any one 5R symmetrical parallel mechanism. The MIC radius atlas of the mechanism with the "+ −" working mode and the up-configuration is presented. Based on the atlas and the usable workspace shape chart, it is very easy for a reader to know the workspace characteristic of a mechanism. Finally, the relationship between the workspace of a non-dimensional mechanism and that of its similarity mechanism with dimension is given. The relationship makes it possible to achieve the optimum result with respect to a desired workspace when an optimum non-dimensional mechanism is obtained based on the atlas. The result in this paper is useful not only for realizing the singularity and workspace performances but for the optimum design of the mechanism as well.

2. Kinematic problems

The planar 5R parallel mechanism, as shown in Fig. 1(a), is such a mechanism that the output point is connected to the base by two legs, each of which consists of three revolute joints and two links. The two legs are connected to a common point with the common revolute joint at the end of each leg. In each of the two legs, the revolute joint connected to the base is actuated. Such a mechanism can position a point freely in a plane.

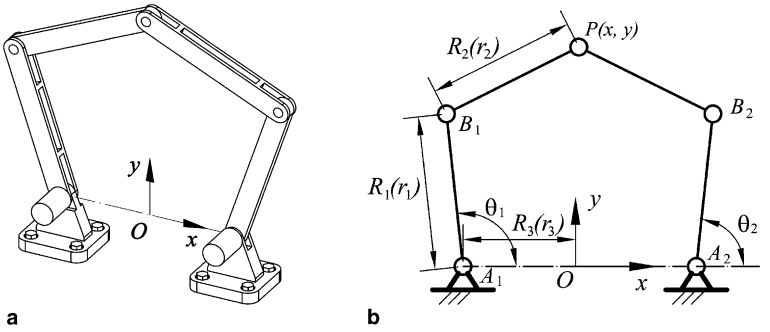

Fig. 1. The planar 5R parallel mechanism.

A kinematics model of the mechanism is developed as shown in Fig. 1(b). Each actuated joint is denoted as A_i ($i = 1,2$), the other end of each actuated link is denoted as B_i and the common joint of the two legs is denoted as P, which is also the output point. A fixed global reference system O–xy is located at the center of A_1A_2 with the y-axis normal to A_1A_2 and the x-axis directed along A_1A_2. For the structure symmetry, there are $OA_1 = OA_2$, $A_1B_1 = A_2B_2$ and $B_1P = B_2P$. The length of the actuated link for each leg is denoted as $A_iB_i = R_1(r_1)$. Additionally, $B_iP = R_2(r_2)$ and $OA_i = R_3(r_3)$. Here, R_j ($j = 1,2,3$) are link lengths with dimension and r_j ($j = 1,2,3$) are those with non-dimension.

2.1. Inverse kinematics

The position of the output point P in the reference system O–xy can be described by the position vector $\boldsymbol{p}$, and there is

$$\boldsymbol{p} = (x \quad y)^{\mathrm{T}} \tag{1}$$

In the reference frame O–xy, the position vectors $\boldsymbol{b}_i$ of points B_i ($i = 1,2$) can be written as

$$\boldsymbol{b}_1 = (r_1\cos\theta_1 - r_3 \quad r_1\sin\theta_1)^{\mathrm{T}} \quad \text{and} \quad \boldsymbol{b}_2 = (r_1\cos\theta_2 + r_3 \quad r_1\sin\theta_2)^{\mathrm{T}} \tag{2}$$

where θ_1 and θ_2 are the input angles of the two legs. Then, the inverse kinematic problem can be solved by writing following constraint equation

$$|\boldsymbol{p}\boldsymbol{b}_i| = r_2, \quad i = 1,2 \tag{3}$$

in another form

$$(x - r_1\cos\theta_1 + r_3)^2 + (y - r_1\sin\theta_1)^2 = r_2^2 \tag{4}$$

$$(x - r_1\cos\theta_2 - r_3)^2 + (y - r_1\sin\theta_2)^2 = r_2^2 \tag{5}$$

from which, if the position of output point P is known, the inputs to reach the position can be obtained as

$$\theta_i = 2\tan^{-1}(z_i), \quad i = 1,2 \tag{6}$$

where

$$z_i = \frac{-b_i + \sigma_i\sqrt{b_i^2 - 4a_ic_i}}{2a_i}, \quad i = 1, 2 \tag{7}$$

in which

$$\sigma_i = 1 \text{ or } -1$$
$$a_1 = r_1^2 + y^2 + (x + r_3)^2 - r_2^2 + 2(x + r_3)r_1$$
$$b_1 = -4yr_1$$
$$c_1 = r_1^2 + y^2 + (x + r_3)^2 - r_2^2 - 2(x + r_3)r_1$$
$$a_2 = r_1^2 + y^2 + (x - r_3)^2 - r_2^2 + 2(x - r_3)r_1$$
$$b_2 = b_1 = -4yr_1$$
$$c_2 = r_1^2 + y^2 + (x - r_3)^2 - r_2^2 - 2(x - r_3)r_1$$

From Eq. (7), one can see that there are four solutions for the inverse kinematic problem of the 5R mechanism. The configuration shown in Fig. 1 can be obtained if $\sigma_1 = 1$ and $\sigma_2 = -1$. Such a configuration is denoted as the "+ −" model. Then there are three others, which are "− +", "− −", and "++" models, respectively. These four inverse kinematics models correspond to four types of working modes.

2.2. Forward kinematics

The forward kinematic problem is to obtain the output with respect to a set of given inputs. From Eqs. (4) and (5), one obtains

$$x^2 + y^2 - 2(r_1\cos\theta_1 - r_3)x - 2r_1\sin\theta_1 y - 2r_1r_3\cos\theta_1 + r_3^2 + r_1^2 - r_2^2 = 0 \tag{8}$$
$$x^2 + y^2 - 2(r_1\cos\theta_2 + r_3)x - 2r_1\sin\theta_2 y + 2r_1r_3\cos\theta_2 + r_3^2 + r_1^2 - r_2^2 = 0 \tag{9}$$

Eq. (8) − (9) yields

$$x = ey + f \tag{10}$$

in which $e = \frac{r_1(\sin\theta_1 - \sin\theta_2)}{2r_3 + r_1\cos\theta_2 - r_1\cos\theta_1}$ and $f = \frac{r_1r_3(\cos\theta_2 + \cos\theta_1)}{2r_3 + r_1\cos\theta_2 - r_1\cos\theta_1}$. Substituting Eq. (10) to Eq. (8) yields

$$dy^2 + gy + h = 0 \tag{11}$$

where

$$d = 1 + e^2$$
$$g = 2(ef - er_1\cos\theta_1 + er_3 - r_1\sin\theta_1)$$
$$h = f^2 - 2f(r_1\cos\theta_1 - r_3) - 2r_1r_3\cos\theta_1 + r_3^2 + r_1^2 - r_2^2$$

Then, y can be obtained from Eq. (11) as

$$y = \frac{-g + \sigma\sqrt{g^2 - 4dh}}{2d} \tag{12}$$

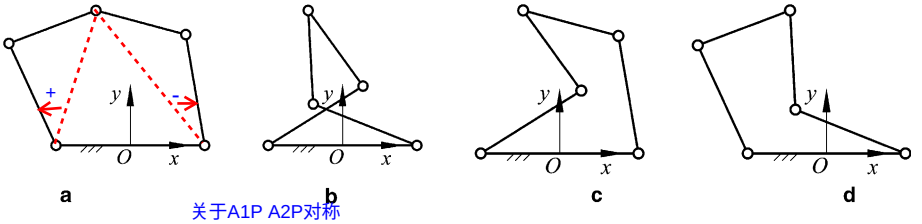

Fig. 2. The four inverse kinematic models: (a) "+ − " model; (b) "− +" model; (c) "− −" model and (d) "++" model.

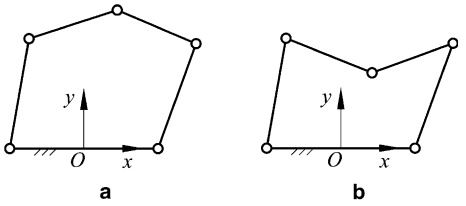

Fig. 3. The two forward kinematic models: (a) the up-configuration and (b) the down-configuration.

in which $\sigma = 1$ or -1. From Eqs. (10) and (12), one sees that there are two solutions for the forward kinematic problem of the mechanism. They corresponds to types of assembly modes. The corresponding configurations are called the *up-* and *down-configurations*. The *up-configuration* can be achieved when $\sigma = 1$.

For example, if $r_1 = 1.2$, $r_2 = 1.0$ and $r_3 = 0.8$, the four inverse kinematic models of the mechanism are shown in Fig. 2, where the specified position of the output point is $(x = -0.37, y = 1.44)$. And the two forward kinematic models are shown in Fig. 3, where the inputs are given as $\theta_1 = 4\pi/9$ and $\theta_2 = 7\pi/18$.

In this paper, what we are concerned about is the mechanism with the "+ −" model and, at the same time, the *up-configuration*.

3. Theoretical workspace

Theoretical workspace is defined as the region that the output point can reach if θ_i changes from 0 to 2π without the consideration of interference between links and the singularity.

From Eq. (4), one can see that if θ_1 is specified, the workspace of the first leg is a circle centered at the point $(r_1 \cos\theta_1 - r_3, r_1 \sin\theta_1)$ with a radius of r_2. The circle is denoted as C_{11}. If θ_i changes from 0 to 2π, the center point is located at a circle centered at point $A_1(-r_3, 0)$ with a radius of r_1. The circle is denoted as C_{12}. Then, the workspace of the leg is the enveloping region of the circle C_{11} when its center rolls at the circle C_{12}. Actually, the enveloping region is an annulus bounded by two following circles:

$$C_{1o} : (x + r_3)^2 + y^2 = (r_1 + r_2)^2 \tag{13}$$

$$C_{1i} : (x + r_3)^2 + y^2 = (r_1 - r_2)^2 \tag{14}$$

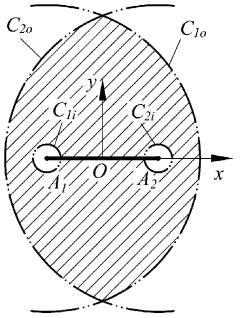

Fig. 4. The theoretical workspace is shown as the hatched region.

For the second leg, the workspace is an annulus bounded by circles

$$C_{2o} : (x - r_3)^2 + y^2 = (r_1 + r_2)^2 \tag{15}$$

$$C_{2i} : (x - r_3)^2 + y^2 = (r_1 - r_2)^2 \tag{16}$$

When $r_1 = r_2$ the workspaces are two circles defined by Eqs. (13) and (15), respectively. The theoretical workspace of the mechanism is the intersection of the two annuluses. For example, the workspace of a mechanism with $r_1 = 1.2$, $r_2 = 1.0$ and $r_3 = 0.8$ is shown as the hatched region in Fig. 4, where the boundaries are also illustrated.

From above analysis, one can see that if $r_3 > r_1 + r_2$, there is no intersection, i.e., no workspace. Especially, if $r_3 = r_1 + r_2$, the workspace is only one point, which is the center of the line segment A_1A_2.

4. Jacobian matrix

Eqs. (4) and (5) can be differentiated with respect to time to obtain the velocity equations, which yields

$$r_1[y\cos\theta_1 - (x + r_3)\sin\theta_1]\dot{\theta}_1 = (x + r_3 - r_1\cos\theta_1)\dot{x} + (y - r_1\sin\theta_1)\dot{y} \tag{17}$$

$$r_1[y\cos\theta_2 + (r_3 - x)\sin\theta_2]\dot{\theta}_2 = (x - r_3 - r_1\cos\theta_2)\dot{x} + (y - r_1\sin\theta_2)\dot{y} \tag{18}$$

Rearranging Eqs. (17) and (18) leads to an equation of the form

$$\boldsymbol{A}\dot{\boldsymbol{\theta}} = \boldsymbol{B}\dot{\boldsymbol{p}} \tag{19}$$

where $\dot{\boldsymbol{p}}$ is the vector of output velocities defined as

$$\dot{\boldsymbol{p}} = (\dot{y} \quad \dot{z})^{\mathrm{T}} \quad [\dot{x} \quad \dot{y}]^T \tag{20}$$

and $\dot{\boldsymbol{\theta}}$ is the vector of input velocities defined as

$$\dot{\boldsymbol{\theta}} = (\dot{\theta}_1 \quad \dot{\theta}_2)^{\mathrm{T}} \tag{21}$$

Matrices $\boldsymbol{A}$ and $\boldsymbol{B}$ are, respectively, the 2×2 matrices of the mechanism and can be expressed as

$$\boldsymbol{A}=\begin{bmatrix} y\cos\theta_1-(x+r_3)\sin\theta_1 & 0 \\ 0 & y\cos\theta_2+(r_3-x)\sin\theta_2 \end{bmatrix}\boldsymbol{r}_1 \tag{22}$$

$$\boldsymbol{B}=\begin{bmatrix} x+r_3-r_1\cos\theta_1 & y-r_1\sin\theta_1 \\ x-r_3-r_1\cos\theta_2 & y-r_1\sin\theta_2 \end{bmatrix} \tag{23}$$

The Jacobian matrix of the mechanism can be written as

$$\boldsymbol{J}=\boldsymbol{A}^{-1}\boldsymbol{B} \tag{24}$$

5. Singularity analysis

In the parallel mechanism, singularities occur whenever $\boldsymbol{A}$, $\boldsymbol{B}$ or both, become singular. As a singularity leads to an instantaneous change of the mechanism's DoF, the analysis of parallel mechanisms has drawn considerable attention.

The singularity of the 5R symmetrical parallel mechanism has been studied by many researchers. Here, we summarize this issue as following.

(1) The stationary singularity occurs when $\boldsymbol{A}$ becomes singular but $\boldsymbol{B}$ remains invertible. Physically, this corresponds to the configuration whenever one of the legs A_1B_1P and A_2B_2P is completely extended or folded. From the analysis of the workspace, this singularity occurs when the output point P reaches its limit or is at the boundary of the workspace. This singularity is also referred to as the *serial singularity*. For example, for the mechanism with the parameters $r_1 = 1.2$, $r_2 = 1.0$ and $r_3 = 0.8$, some configurations of this kind of singularity are shown in Fig. 5. The loci of this kind of singularity are actually given by circles C_{1o}, C_{1i}, C_{2o} and C_{2i}, as shown in Fig. 4. Note that, $r_1 = 0$ leads to $\det(\boldsymbol{A}) = 0$ as well. But this also results the mechanism in an immovable status.

$$(a,b):\ tan\theta_1=\frac{y}{x+r_3}\rightarrow a_{11}=0\rightarrow \det(A)=0$$

$$(c,d):\ tan\theta_2=\frac{y}{r_3-x}\rightarrow a_{22}=0\rightarrow \det(A)=0$$

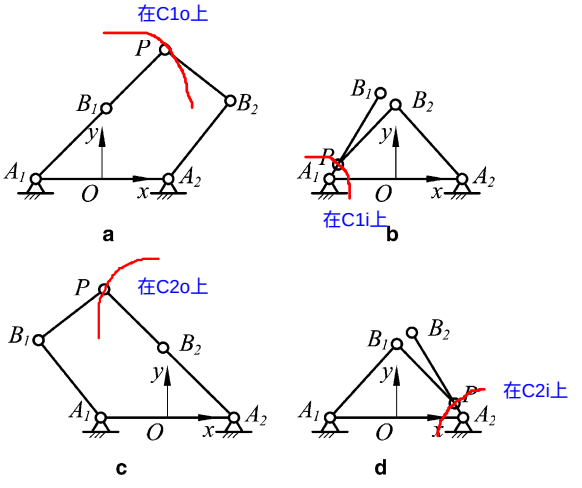

Fig. 5. Some configurations of the stationary singularity: (a) the first leg is completely extended; (b) the first leg is completely folded; (c) the second leg is completely extended and (d) the second leg is completely folded.

(2) The uncertainty singularity, occurring only in closed kinematics chains, arises when $\boldsymbol{B}$ becomes singular but $\boldsymbol{A}$ remains invertible. Usually, there are two cases for this singularity. The first case is that B_1PB_2 is completely folded, i.e., the points B_1 and B_2 are coincident. Such a configuration is shown in Fig. 6(a), from which one can see that when this condition occurs the locus of the point P is a circle centered at point $\left(0, \sqrt{r_1^2 - r_3^2}\right)$ or $\left(0, -\sqrt{r_1^2 - r_3^2}\right)$ with a radius of r_2, namely,

$$x^2 + \left(y - \sqrt{r_1^2 - r_3^2}\right)^2 = r_2^2 \quad \text{or} \quad x^2 + \left(y + \sqrt{r_1^2 - r_3^2}\right)^2 = r_2^2 \tag{25}$$

Please note that, if $r_3 = 0$, this type of singularity can occur easily when links A_1B_1 and A_2B_2 are coincident as shown in Fig. 6(b). For this case, the loci of point P is an annulus, which is bounded by two circles

$$x^2 + y^2 = (r_1 + r_2)^2 \quad \text{and} \quad x^2 + y^2 = (r_1 - r_2)^2 \tag{26}$$

The second case is that when B_1PB_2 is completely extended. Such a singular configuration is shown in Fig. 7. The locus of point P for this type of singularity can be described by

$$\begin{cases} x = r_1(\cos\theta_2 + \cos\theta_1)/2 \\ y = r_1(\sin\theta_2 + \sin\theta_1)/2 \end{cases} \tag{27}$$

无数个正解，P点受外力影响

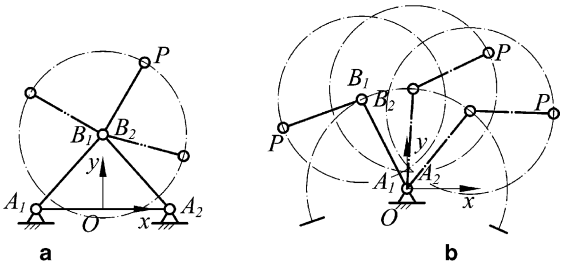

Fig. 6. The configurations when B_1 and B_2 are coincident.

在Type 2类奇异点处.θ1固定，θ2增加
下一个位置是Up/Down是无法确定的

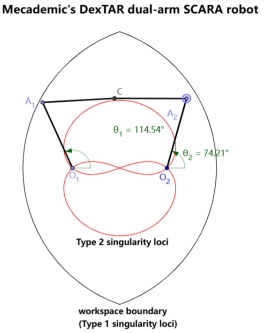

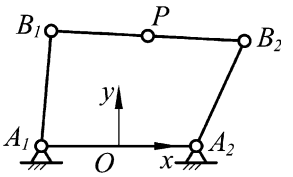

Up,Down Configuration 重合，正解个数=1

Fig. 7. The configuration when B_1PB_2 is completely extended.

where

$$\theta_1 \in [0, 2\pi]$$

$$\theta_2 = 2\tan^{-1}(z)$$

$$z = \left(-b \pm \sqrt{b^2 - 4ac}\right)/(2a)$$

$$a = 4r_2^2 + 4r_1 r_3 \cos\theta_1 + 4r_1 r_3 - 4r_3^2 - 2r_1^2 - 2r_1^2 \cos\theta_1$$

$$b = 4r_1^2 \sin\theta_1$$

$$a = 4r_2^2 + 4r_1 r_3 \cos\theta_1 - 4r_1 r_3 - 4r_3^2 - 2r_1^2 + 2r_1^2 \cos\theta_1$$

Based on the analysis in [23], Eq. (27) can be also rewritten as the following sextic:

$$(x + 2r_3)^2(x^2 + 4r_3x + 3r_3^2 + r_2^2 - r_1^2 + y^2)^2 + y^2(x^2 + 4r_3x + 5r_3^2 + r_2^2 - r_1^2 + y^2)^2 - 4r_3^2 r_2^2 y^2 = 0 \quad (28)$$

图像需要向右平移2*r3　使用(x-2*r3)代替x

For the uncertainty singularity, if $r_1 < r_3$, the singularity that B_1 and B_2 are coincident will not occur. If $r_2 > r_1 + r_3$, there is no the singularity that B_1PB_2 is completely extended.

(3) The third kind of singularity occurs when both $\boldsymbol{A}$ and $\boldsymbol{B}$ become simultaneously singular. This singularity is of a slightly different nature than the first two since it is not only configuration but also architecture dependent.

From the analysis on the stationary and uncertainty singularities, one can see that the third kind of singularity occurs when the five points A_1, B_1, P, B_2 and A_2 are collinear. There are six cases for this kind of singularity, as shown in Fig. 8. The parameter conditions to those singularities are as following:

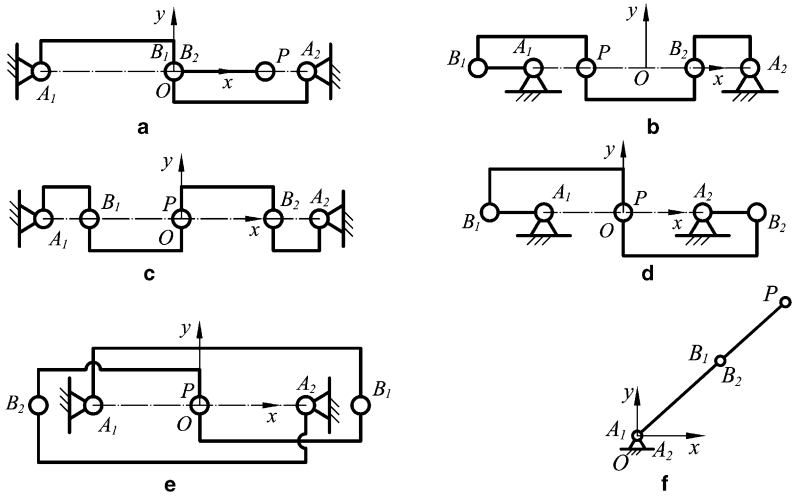

Fig. 8. Six configurations of the third kind of singularity.

(a) $r_1 = r_3$, one singularity is shown in Fig. 8(a);
(b) $r_2 = r_3$, a corresponding singular configuration is shown in Fig. 8(b);
(c) $r_3 = r_1 + r_2$, see Fig. 8(c) for the singular configuration;
(d) $r_2 = r_1 + r_3$, Fig. 8(d) shows such a singularity;
(e) $r_1 = r_3 + r_2$, see Fig. 8(e);
(f) $r_3 = 0$, one singular configuration is shown in Fig. 8(f).

The mechanism satisfies any one of the five parameter conditions (a)–(e) is referred to as *a change point mechanism*.

The analysis on the kinematics of the mechanism shows that there are four solutions for the inverse kinematics and two solutions for the forward kinematics. Any one of the singularities will result in the change of solution number of the kinematics. For example, the stationary singularity leads to the loss of solution number of the inverse kinematics. While in the uncertainty singular configuration, the solution number of the forward kinematics can be less or more than two. In the third kind of singularity, both the inverse and forward kinematics will be different. Then the stationary singularity can be called the inverse kinematic singularity, the uncertainty singularity the forward kinematic singularity, and the third kind of singularity the inverse and forward kinematic singularity. Notably, the loci of the uncertainty singularity must be within the workspace.

6. The design space of the 5R parallel mechanism

As it is well-known, the performance of a parallel mechanism depends on not only the pose of the moving platform but also the link lengths (dimensions). Disregarding the pose, each of the links can be the length between zero and infinite. And there are always several links in a parallel mechanism. Then the combination of the links with different lengths will be infinite. They undoubtedly have different performance characteristics. To apply a specified mechanism in practice, we usually should determine the link lengths with respect to a desired application. This is actually the so-called optimum design (parameter synthesis) of the mechanism. In such a process, one of the most classical tools that has been using is the chart, which can show the relationship between performances and link lengths. To make it work, we should first develop a space that contains all involved links. Next is to plot the chart considering a desired performance. In this paper, the space is referred to as *the design space*. The chart that can show the relationship between performances and link lengths is referred to as *atlas*. The *index* is used to evaluate a performance. Normally, several indices will be considered in the design process.

For the parallel mechanism considered here, due to the symmetric structure, there leaves three parameters, which are R_1, R_2 and R_3 as shown in Fig. 1. Any one of the parameters R_1, R_2 and R_3 can have any value between zero and infinite. This is the biggest difficulty to develop a design space that can embody all mechanisms (with different link lengths) within a finite space. For this reason, we must eliminate the physical link size of the mechanisms. Let

$$D = (R_1 + R_2 + R_3)/3 \tag{29}$$

One can obtain three non-dimensional parameters r_i by means of

$$r_1 = R_1/D, \quad r_2 = R_2/D, \quad r_3 = R_3/D \tag{30}$$

This would then yield

$$r_1 + r_2 + r_3 = 3 \qquad (31)$$

r1 r2 r3无量纲， 等于3倍的百分比

Theoretically, from Eq. (31), the three non-dimensional parameters r_1, r_2 and r_3 can have any value between 0 and 3. For the 5R parallel mechanism studied here, the analysis on the workspace and singularity shows that r_1 and r_2 cannot be 0 and $r_1 + r_2$ cannot be less than r_3, otherwise they will result in the failure of mechanism assembly. Therefore, the three parameters should be

$$0 < r_1, r_2 < 3 \quad \text{and} \quad 0 \leqslant r_3 \leqslant 1.5 \qquad (32)$$

Based on Eqs. (31) and (32), one can establish a design space as shown in Fig. 9(a), in which the trapezoid $ABCD$ is actually the design space. In Fig. 9(a), the trapezoid $ABCD$ is restricted by r_1, r_2 and r_3. Therefore it can be figured in another form as shown in Fig. 9(b), which is referred to as the planar-closed configuration of the design space.

For convenience, two orthogonal coordinates s and t are utilized to express r_1, r_2 and r_3. Thus, by using

$$\begin{cases} s = 2r_1/\sqrt{3} + r_3/\sqrt{3} \\ t = r_3 \end{cases} \qquad (33)$$

容易验证C(0,3,0)对应{st}的原点
B(3,0,0)在s轴正方向上
t轴对应s=0 2r1+r3 = 0, 与r1+r2+r3=3在P(1,4,-2)处相交。
容易验证CP ⊥BC

coordinates r_1, r_2 and r_3 can be transformed into s and t. Eq. (33) is useful for constructing a performance atlas.

In order to study the performance of the parallel mechanism in detail, five lines $r_1 = r_3$, $r_2 = r_3$, $r_2 = r_1 + r_3$, $r_1 = r_3 + r_2$ and $r_1 = r_2$ can be used to divide the design space into 10 sub-regions, i.e., Ia, Ib, IIa, IIb, IIIa, IIIb, IVa, IVb, Va and Vb, as shown in Fig. 9(b). The former four lines indicate four types of change point mechanisms, respectively. The reason why $r_1 = r_2$ is also used is that if $r_1 = r_2$ the boundaries of the theoretical workspace are only two circles C_{1o} and C_{2o}. Such a design space will help us to investigate detailedly the performance characteristics of all 5R parallel mechanisms with possible combinations of $R_1(r_1)$, $R_2(r_2)$ and $R_3(r_3)$.

We would like to mention that the concept using non-dimensional parameters to establish a finite space of a parallel mechanism was introduced in [15,17,20], where the space is defined as *the physical model of the solution space*, which was used to study some performances of the 5R parallel mechanism. The performances were based on the theoretical workspace without the

ABCD四点坐标已知。
AC直线上的点通过向量共线可得出
r1=r3

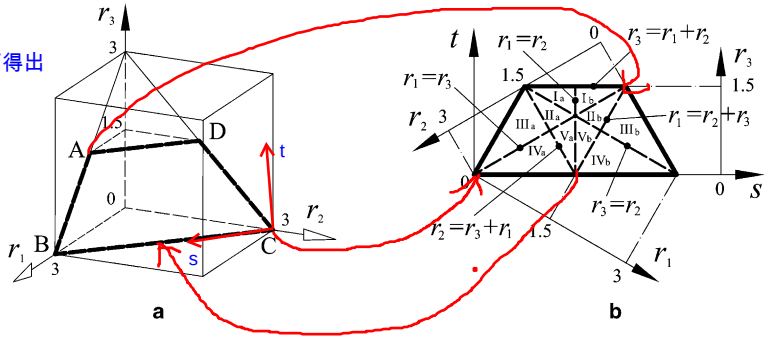

Fig. 9. The design space of the 5R parallel mechanism.

consideration of singularity. For example, according to the result in [17,20], the atlas of global conditioning index for the mechanism with the working mode "+ −" is the same as that of the mechanism with "− +" mode. But the analysis in this paper will show that the singular loci and workspace without singularity will be different for different working modes. Then, the atlases should not be the same. For such a reason, practically, the obtained atlases in the references cannot be used directly by readers. In this paper, the singularity will be taken into account throughout the evaluation of the performances and the optimum design of the parallel mechanism. Then, the result of the paper will be more precisely and can be referred by others. What is more, the design space established here is a little different from the solution space used in [17,20]. One can see that the three parameters used here are easier to be accepted to present the change point mechanisms and classify the mechanisms.

7. Theoretical workspace

7.1. Atlas of the workspace area

The theoretical workspace can be determined based on Eqs. (13)–(16). The workspace area can be calculated following the equations given in [15,20]. The atlas for the theoretical workspace area is shown in Fig. 10, from which one can see that

- The theoretical workspace area is inverse proportional to parameter r_3.
- The area atlas is symmetric with respect to $r_1 = r_2$, which means that the area of a mechanism with $r_1 = a$, $r_2 = b$ $(a, b < 3)$ and $r_3 = 3 - a - b$ is identical to that of a mechanism with $r_1 = b$, $r_2 = a$ $(a, b < 3)$ and $r_3 = 3 - a - b$.
- When $r_3 = 1.5$ (or $r_1 + r_2 = r_3$), the area is 0.
- The area reaches its maximum value when $r_1 = r_2 = 1.5$ and $r_3 = 0$. The maximum value is 9π.

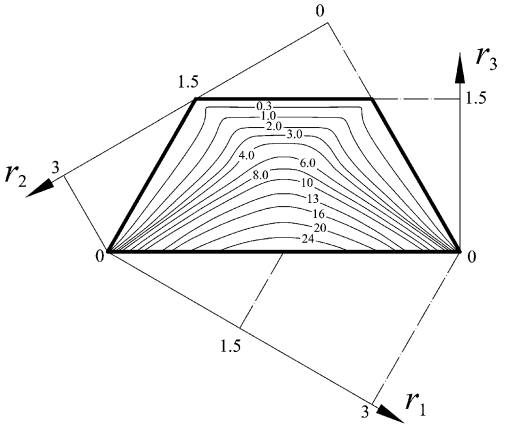

Fig. 10. The atlas of the theoretical workspace area.

7.2. Distribution characteristics of the theoretical workspace shape in the design space

Meanwhile, we can also obtain the workspace of a typical mechanism in each of the 10 subregions. The distribution characteristics of the workspace shape can be summarized based on these workspaces. The distribution in the design space is shown in Fig. 11, from which one can see that the distribution is symmetric with respect to the line $r_1 = r_2$. This means that the theoretical workspace shape of a mechanism with $r_1 = a$, $r_2 = b$ $(a, b < 3)$ and $r_3 = 3 - a - b$ is the same as that of a mechanism with $r_1 = b$, $r_2 = a$ $(a, b < 3)$ and $r_3 = 3 - a - b$. This characteristic is what it should be, as the radii of boundary circles C_{1o}, C_{2o}, C_{1i} and C_{2i} of the theoretical workspace are just related to $r_1 + r_2$ and $|r_1 - r_2|$. Then there are only five types of theoretical workspace shapes for the 5R parallel mechanism. What is more, each theoretical workspace is symmetric about the x and y axes.

8. Distribution characteristics of singular loci in the design space

Based on the analysis on the singularity, there exist two kinds of singular loci. The first kind of locus is the inverse singular locus. The loci are C_{1o}, C_{1i}, C_{2o} and C_{2i} given by Eqs. (13)–(16). They are actually the boundaries of the theoretical workspace. The second one is the forward singular locus. There are two cases for this kind of singular locus. One is that when the points B_1 and B_2 are coincident. The loci are actually two circles given by Eq. (25), which are denoted as $C_{\text{Coin-U}}$ and $C_{\text{Coin-D}}$. The second case occurs when B_1PB_2 is completely extended. The locus is presented by Eq. (27) or Eq. (28), which is denoted as C_{Col}.

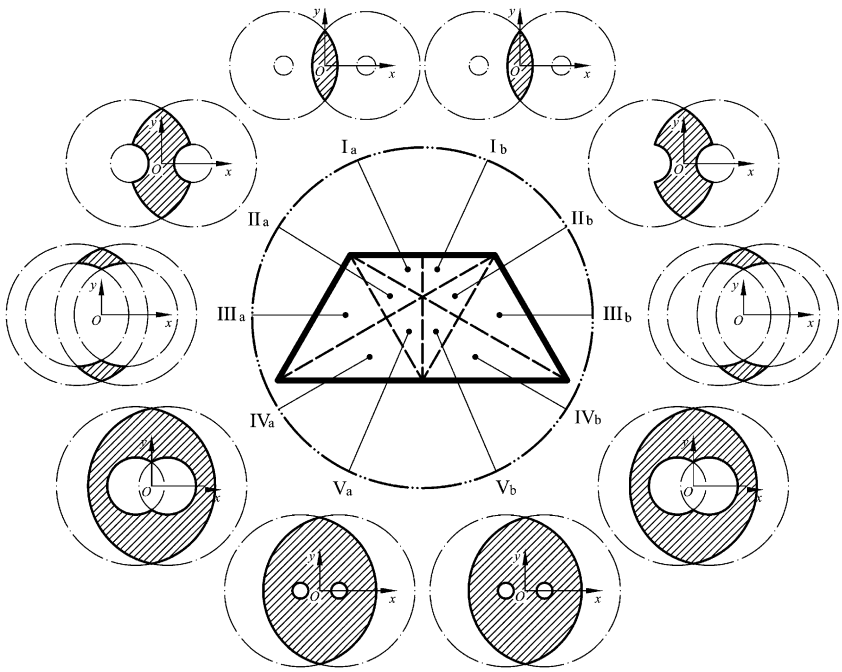

Fig. 11. Distribution of the theoretical workspace shape in the design space.

For example, for the mechanism with $r_1 = 1.2$, $r_2 = 1.0$ and $r_3 = 0.8$, the singular loci are shown in Fig. 12.

The singular loci for the mechanism with different link lengths will be different. They can be illustrated by Fig. 13, from which one can see that

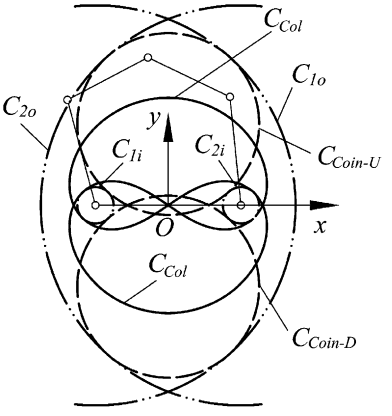

Fig. 12. The singular Loci of a mechanism.

Vb

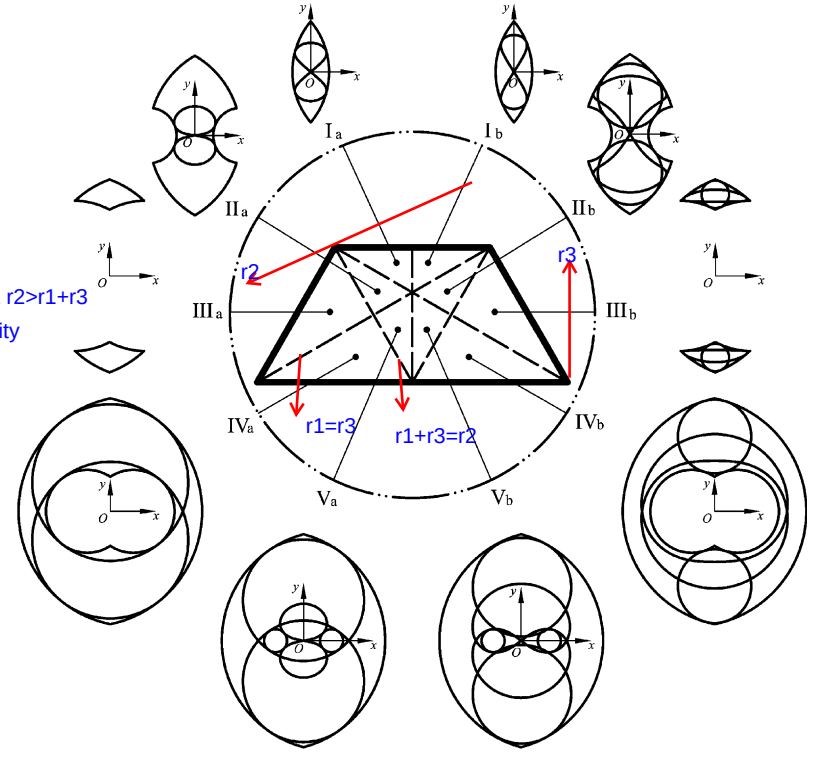

IIIa区域满足:r3>r1 && r2>r1+r3
无uncertainty singularity

Fig. 13. Distribution of singular loci in the design space.

- For a specified mechanism, the distribution of singular loci within the workspace is symmetric about the x and y axes.
- The distribution in the design space is not symmetric with respect to $r_1 = r_2$. This indicates that the singular loci of a mechanism with $r_1 = a$, $r_2 = b$ $(a, b < 3)$ and $r_3 = 3 - a - b$ is not the same as that of a mechanism with $r_1 = b$, $r_2 = a$ $(a, b < 3)$ and $r_3 = 3 - a - b$.
- For the mechanisms in sub-regions Ia, Ib, IIa and IIIa where $r_1 < r_3$, there are no singular loci $C_{\text{Coin-U}}$ and $C_{\text{Coin-D}}$, i.e., no the singular configurations that the points B_1 and B_2 are coincident in their workspaces.
- For the mechanisms in sub-regions IIIa and IVa where $r_1 + r_3 < r_2$, there is no singular locus C_{Col} in their workspaces. For these mechanisms, B_1PB_2 cannot be completely extended.
- The mechanisms in sub-region IIIa where $r_1 < r_3$ and $r_1 + r_3 < r_2$ do not have the uncertainty singularity.

As we know, the workspace where a real mechanism works is different from the theoretical workspace. The region should contain no singular loci inside. From the distribution of theoretical workspace area and shape, one can see that the workspace area and shape of the mechanism with parameters $r_1 = 0.7$, $r_2 = 1.3$ and $r_3 = 1.0$ are identical to those of the mechanism with parameters $r_1 = 1.3$, $r_2 = 0.7$ and $r_3 = 1.0$. But from the analysis on singularity, the singularity loci for these two mechanisms are different. This will directly result in different usable workspaces. Therefore, based on Figs. 10 and 11, one cannot give any design result for a practical mechanism.

9. The usable workspace

9.1. Definition

As there exist singular loci inside the theoretical workspace, a mechanism wants to move from one point to another it maybe should pass a singular configuration. That means it should change from one working mode to another. In practice, changing working mode during the working process is definitely impossible. Therefore, we should find out a working space without singularity.

The *usable workspace* is defined as the maximum continuous workspace that contains no singular loci inside but bounded by singular loci outside. According to this definition, not every point within the usable workspace can be available for a practical mechanism. The mechanism will be out of control at the points on the boundaries and their neighborhoods. But within this region, the mechanism with a specified working mode can move freely.

In Section 8, the first and second kinds of singular loci have been presented for the mechanism in each sub-region as shown in Fig. 13. The stationary singularity is actually the boundary of a theoretical workspace. Then, a mechanism with every working mode can have such singular loci. However, as the uncertainty singularity occurs inside the workspace, not every working mode has all such singularities. Normally, for most 5R parallel mechanisms, there are four tangent points between the first and second kinds of singular loci. At these points, the mechanism is in the change point's mechanism. The points can be used to identify which singular loci a specified working mode can have. For example, all singular loci of the mechanism $r_1 = 1.2$, $r_2 = 1.0$ and $r_3 = 0.8$ are shown in Fig. 12. And Fig. 14 shows some singular configurations and singular loci of the

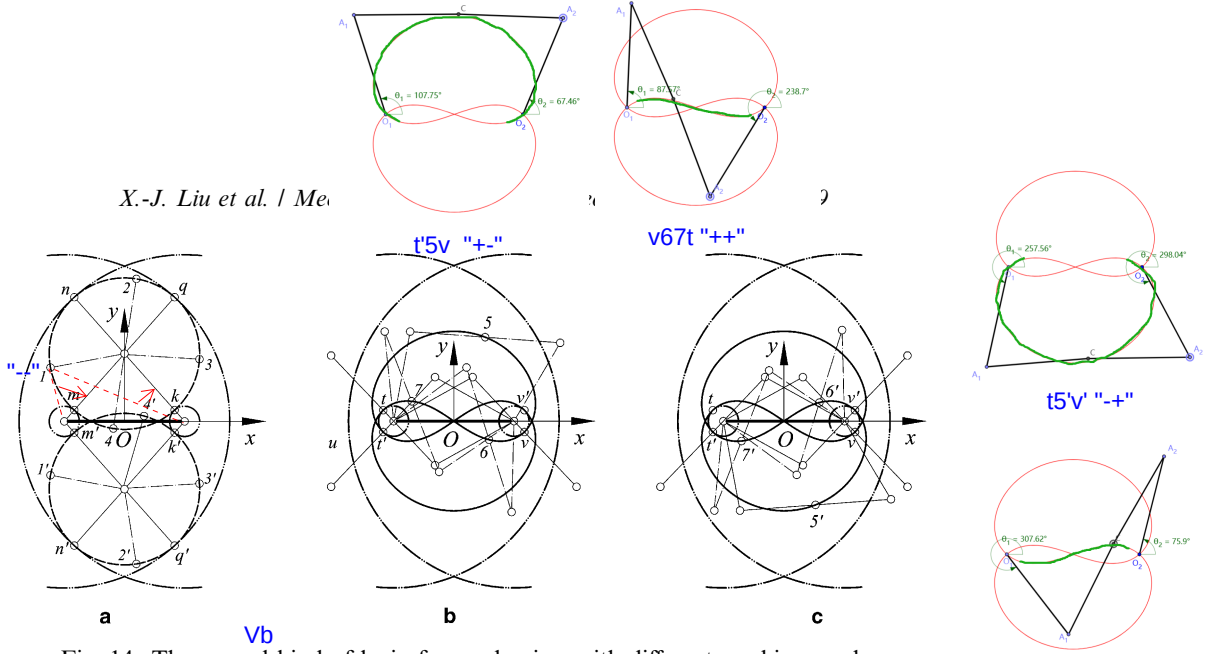

Fig. 14. The second kind of loci of a mechanism with different working modes.

B1B2重合,P绕B1旋转,显然有4个切点。同时A1 m B1 q 四点共线, A2 k B1 n 四点共线。

mechanism. As shown in Fig. 14 (a), there are four tangent points m, n, q and k between the singular curve $C_{\text{Coin-U}}$ and the first kind of singular loci. At these four points, both of the stationary and uncertainty singularities occur. The four points divide the singular curve $C_{\text{Coin-U}}$ into four parts. At the arc $m1n$, the mechanism is in singular only when it is with the "− −" mode. At the arcs $n2q$, $q3k$ and $k4m$, the working modes "− +", "++" and "+ −" are in singular, respectively. Similarly, at $C_{\text{Coin-D}}$, arcs $m'1'n'$, $n'2'q'$, $q'3'k'$ and $k'4'm'$ are the singular curves for the working modes "++", "+ −", "− −" and "− +", respectively. For the singular locus C_{Col}, as shown in Fig. 14(b) and (c), curves $t5v$, ~~$t76v$~~, $t5'v'$ and ~~$t'7'6'v'$~~ are the singular loci for the working modes "+ −", "++", "− +" and "− −", respectively. For the mechanisms in sub-region IVb where $r_1 > r_2 + r_3$ and $r_2 > r_3$, the parameter condition does not allow the case that the singular locus C_{Col} and the first kind of singular locus are tangent to occur. These mechanisms with the working modes "++" and "− −" don't have the singularity that B_1PB_2 is completely extended.

逆时针的光滑曲线段, v67t v'6'7't'

In this paper, we are just concerned about the mechanism with the working mode "+ −". Fig. 15 shows the singular loci for all mechanisms with the working mode in the design space.

The singular loci shown in Fig. 15 can be used to determine the usable workspace of a 5R parallel mechanisms with both the working mode "+ −" and the up-configuration. The workspace of a mechanism should be continuous. As shown in Fig. 15, the singular loci divide the theoretical workspace into several regions. The regions for the mechanisms in all sub-regions are separated. A practical mechanism cannot access the singular loci from one region to another. Even though, from Fig. 15, one can see that the two actuated links of the mechanism in sub-regions IVa, IVb, Va and Vb are both crank links. If one wants to find a mechanism that has two actuated crank links and has a surrounding workspace, he can select such a mechanism in these four sub-regions. But, the analysis in paper [22] will show that within the region under the x-axis, the local conditioning index for some mechanisms will be worse. That means only the region above the x-axis will be used in practice. For some mechanisms, there exist several regions with good local conditioning index. ??? However, they are usually separated by the region with bad performance. In order to present a workspace closer to the practical workspace of the mechanism, the usable workspace defined here will not be the whole workspace, especially for the mechanisms in sub-regions IVa, IVb, Va and Vb. What is more, in the workspace under the x-axis, the two actuated links of a mechanism with the working mode "+ −" usually intersect. Practically, we

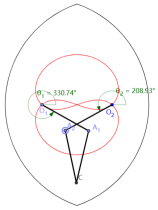

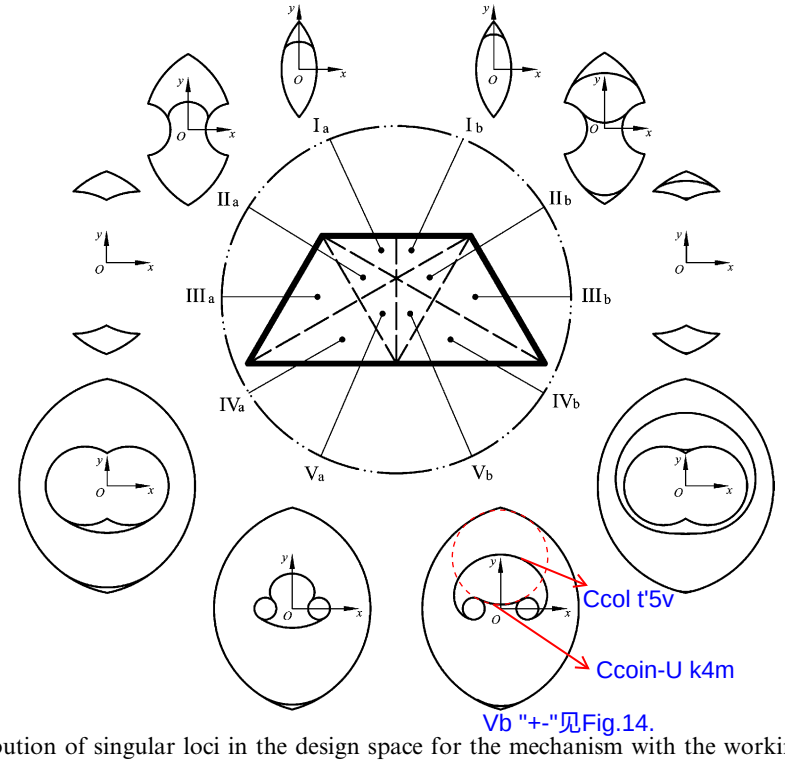

Fig. 15. Distribution of singular loci in the design space for the mechanism with the working mode "+ −".

prefer the configuration as shown in Fig. 1. For such reasons, we define the region above the x-axis as the usable workspace. For example, the usable workspace of the mechanism with $r_1 = 1.2$, $r_2 = 1.0$ and $r_3 = 0.8$ is shown as the hatched region in Fig. 16. Within this workspace, the mechanism has the configuration with both the inverse working mode "+ −" and the forward up-configuration. For the mechanism in one of the sub-regions Ia, Ib, IIa, IIb, IIIa and IIIb, the theoretical workspace above the x-axis is divided by the singular loci into several non-continuous regions, in which the region on the most top, where the mechanism is with the up-configuration, is considered as its usable workspace by taking into account the reasons mentioned above.

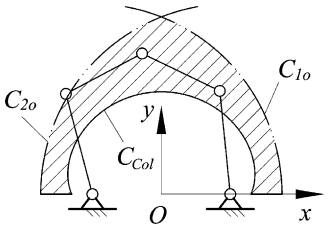

Fig. 16. The usable workspace of a mechanism.

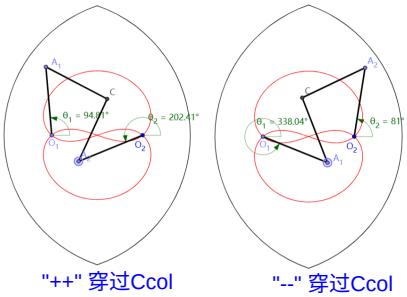

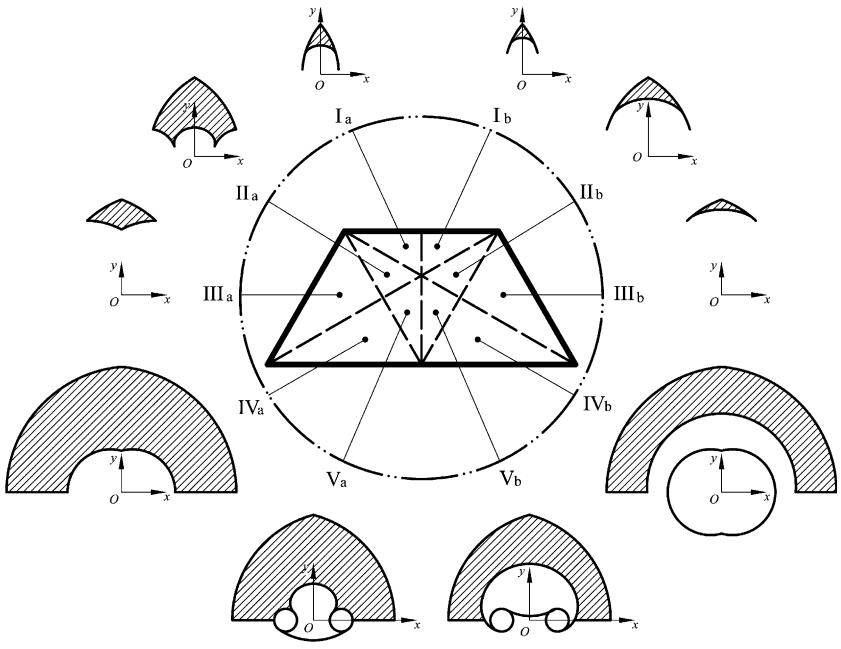

Fig. 17. The usable workspace shape in the design space.

9.2. Distribution of the usable workspace shape in the design space

The usable workspace shape for the 5R parallel mechanism is classified in the design space as shown in Fig. 17. From the distribution one sees that

- In Fig. 17, each of the hatched regions is the usable workspace of the mechanism with the "+ −" working mode and the up-configuration, simultaneously.
- Each usable workspace is symmetric about the y-axis.
- The distribution in the design space is not symmetric about $r_1 = r_2$. The usable workspace shape of a mechanism with $r_1 = a$, $r_2 = b$ $(a, b < 3)$ and $r_3 = 3 - a - b$ is no longer the same as that of a mechanism with $r_1 = b$, $r_2 = a$ $(a, b < 3)$ and $r_3 = 3 - a - b$.
- The usable workspace of a mechanism in sub-region IVa is half of its theoretical workspace.
- The flattest part in the workspace is always located at the region where $y = 0$.

10. The maximal inscribed circle (MIC) and the maximal inscribed workspace (MIW)

10.1. Definition

In the design process, in order to make the workspace of a device as large as possible and as far away from the singularity as possible, we usually select the thickest part in the usable workspace as our research object. As shown in Fig. 17, the thickest part is always symmetric about the y-axis.

It can be characterized by a circle, which is tangent with the singular loci. Here, the circle is referred to as the MIC, which is defined as the circle that is located at the y axis and is tangent with the usable workspace boundary curves. The significance of MIC will be explained further in [22]. According to this definition, the MIC can be described as

$$x^2 + (y - y_{\mathrm{MIC}})^2 = r_{\mathrm{MIC}}^2 \tag{34}$$

where r_{MIC} is the radius and $(0, y_{\mathrm{MIC}})$ is the center. Based on the analysis of the usable workspace, for the mechanisms in sub-regions IIIa and IVa where $r_1 + r_3 < r_2$, the MIC should be tangent with the circles $C_{1\mathrm{o}}$, $C_{1\mathrm{i}}$, $C_{2\mathrm{o}}$ and $C_{2\mathrm{i}}$. For this case, the radius and y_{MIC} of the MIC can be given as

$$r_{\mathrm{MIC}} = (r_1 + r_2 - |r_1 - r_2|)/2 \quad \text{and} \quad y_{\mathrm{MIC}} = \sqrt{(r_1 + r_2 + |r_1 - r_2|)^2/4 - r_3^2} \tag{35}$$

For the mechanisms in the other sub-regions where $r_1 + r_3 > r_2$ in the design space, the MIC should be tangent with $C_{1\mathrm{o}}$, $C_{2\mathrm{o}}$ and C_{Col}. What is more, for this case, the MIC is actually the circle that passes through the intersect point between C_{Col} and the y-axis and is tangent with $C_{1\mathrm{o}}$ and $C_{2\mathrm{o}}$. Its radius and y_{MIC} can be expressed as

$$r_{\mathrm{MIC}} = |y_{\mathrm{MIC}}| - y_{\mathrm{Col}} \quad \text{and} \quad y_{\mathrm{MIC}} = [(r_1 + r_2 + y_{\mathrm{Col}})^2 - r_3^2]/2(r_1 + r_2 + y_{\mathrm{Col}}) \tag{36}$$

where $y_{\mathrm{Col}} = \sqrt{r_1^2 - (r_2 - r_3)^2}$.

10.2. Distribution of the MIC radius in the design space and the atlas of MIW area

Fig. 18 shows the distribution of the MIC radius in the design space. Fig. 19 shows the atlas of the MIC radius r_{MIC}.

From Fig. 19, one can see that the line $r_1 + r_3 = r_2$ divides the design space into two parts. In the right part, if r_1 is specified the MIC radius is proportional to r_2. In the left part, if r_2 is specified the MIC radius is proportional to r_1. The MIC radius reaches its maximal value 1.5 when $r_1 = r_2 = 1.5$.

From the above analysis, one sees that a usable workspace is an irregular region. In addition, within the usable workspace many points cannot be used by the mechanism in practice since they are near to the singular loci. The MIC is a regular region. Its area is well known as πr_{MIC}^2, which is characterized by the radius r_{MIC}. Such a region circled by the MIC is referred to as the MIW. Although the MIW cannot stand for the exact value of the usable workspace area, its radius atlas shown in Fig. 19 does indicate which mechanism has a larger usable workspace and which one has a smaller workspace with the help of its workspace shape characteristics shown in Fig. 17. In addition, the MIW always stands for the thickest part of the usable workspace. That means in this region there are more points far from the singular curve. Then, the practical workspace of a device will use most of this region. For such a reason, the MIW can characterize the workspace of a practical mechanism (This will be explained further in paper [22]). In the performance analysis, what we are concerned about is usually a comparative result but not the exact value. This is the reason why we give the atlas of the MIC radius instead of the usable workspace area. And, as the definition of most global performance indices is depended on the workspace, the MIW will be used to evaluate the performances.

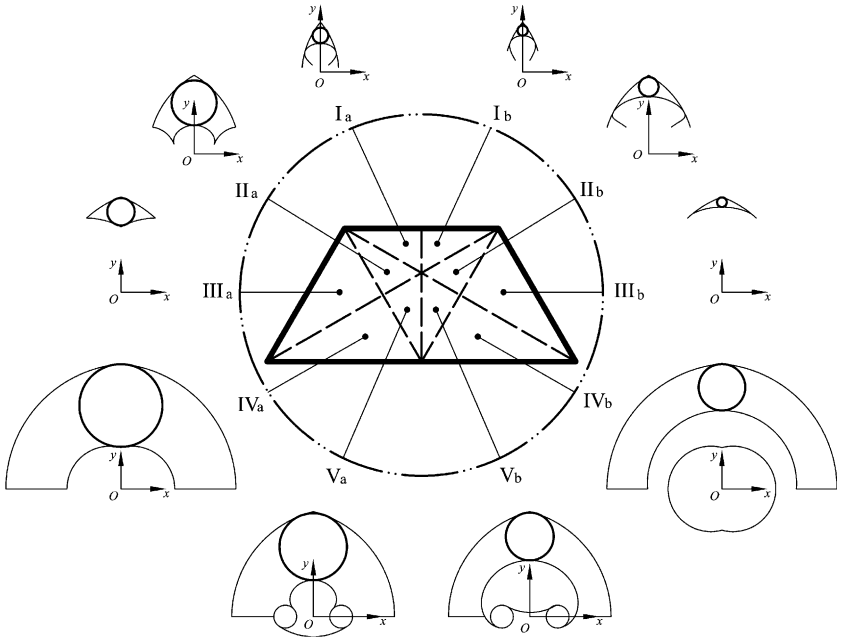

Fig. 18. Distribution of the MIC radius in the design space.

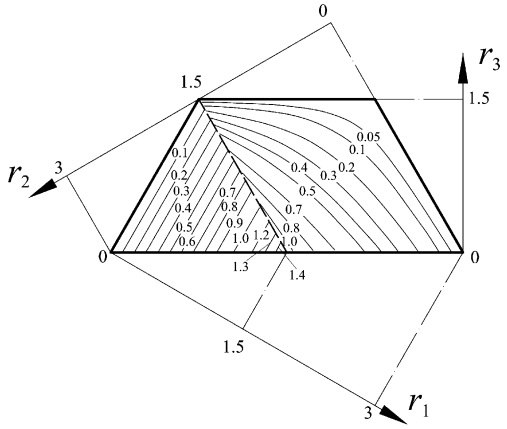

Fig. 19. Atlas of the MIC radius.

Comparing Figs. 17–19 with each other, one can notice that the MIC radius atlas cannot exactly identical with the usable workspace area atlas, which was not plotted. For example, from Fig. 19, there can exist two mechanisms that are in sub-regions IIa and IVb, respectively. They can have same MIC radii. But, from Figs. 17 and 18, one can see that their usable workspace areas will be different. Therefore, before to reach a result on the usable workspace performance of a 5R parallel mechanism, Figs. 17–19 should be used at a same time.

11. The relationship between a non-dimensional mechanism and its corresponding dimensional mechanism

In the design space, the parameters r_1, r_2 and r_3 have no dimension. They are the ratios of the dimensional parameters R_i to a dimensional scale D, which is the average of R_1, R_2 and R_3 as shown in Eq. (29). As given in Eq. (32), the parameters r_1, r_2 and r_3 are limited. But each of the parameters R_1, R_2 and R_3 can be infinite. Practically, we are concerned with the dimensional mechanism but not the non-dimensional one. But it is not difficult to find that the ratio $R_1{:}R_2{:}R_3$ is always equal to $r_1{:}r_2{:}r_3$. For any possible dimension combination of R_1, R_2 and R_3, one can always find its corresponding group of r_1, r_2 and r_3 in the design space. The design space defined by r_1, r_2 and r_3 makes it possible for us to investigate the performance of all possible 5R parallel mechanisms. For example, the atlas of Fig. 19 shows the global result about the MIC radius, which can characterize the usable workspace with the help of Fig. 17 and 18. From Figs. 17–19, we can know the usable workspace result of a non-dimensional 5R parallel mechanism. Then, how about the dimensional mechanisms? We know that the key coefficient between R_i and r_i is the dimensional scale D. Once we select a suitable group of r_1, r_2 and r_3, the parameter D will lead it to a dimensional mechanism by Eq. (30). The problem is how the usable workspace of the dimension mechanism will be if one knows that of a non-dimensional mechanism from Figs. 17–19.

Suppose that R_{MIC} and $(0, Y_{\mathrm{MIC}})$ are the radius and center point of the MIC of a dimensional mechanism. From Eqs. (30), (35) and (36), one can obtain the following result

$$R_{\mathrm{MIC}} = Dr_{\mathrm{MIC}} \quad \text{and} \quad Y_{\mathrm{MIC}} = Dy_{\mathrm{MIC}} \tag{37}$$

Undoubtedly, Eq. (37) indicates that the MIC radius is the result of D times that of its corresponding non-dimensional mechanism. Then, for the MIW and the usable workspace, there should be a D^2-time relationship. The relationship of Eq. (37) can help us to determine the usable workspace of a mechanism based on the results of Figs. 17–19. The relationship also shows that the singular loci of the non-dimensional 5R parallel mechanism and its corresponding dimensional mechanism are identical in the curve shape.

For example, based on Fig. 19 or Eq. (36), one knows that the MIC radius of the non-dimensional mechanism with $r_1 = 1.2$, $r_2 = 1.0$ and $r_3 = 0.8$ is 0.4138. Let $D = 50$ mm, the corresponding dimensional mechanism should be $R_1 = 60$ mm, $R_2 = 50$ mm and $r_3 = 40$ mm. Its MIC radius will then be 20.69 mm and the MIW area is $20.69^2\pi$ mm^2.

Inversely, if one wants to know the singularity and workspace performances of a mechanism with $R_1 = 26$ mm, $R_2 = 30$ mm and $r_3 = 40$ mm, he can do that with respect to Figs. 11, 13, 17–19. Firstly, he should calculate the parameter D using Eq. (29), e.g., here $D = 32$ mm. Then, with Eq. (30), r_1, r_2 and r_3 can be obtained as $r_1 = 0.8125$, $r_2 = 0.9375$ and $r_3 = 1.25$. From Fig. 9(b), as $r_1 < r_2$, $r_1 < r_3$ and $r_2 < r_3$ the mechanism is located in the sub-region Ia. Then, from Fig. 11, he can know the theoretical workspace shape of the mechanism. Fig. 13 can give him the information about the singular loci. And the dimensional mechanism also has such singular loci in its workspace. Fig. 17 shows the usable workspace shape. From these figures, he can learn that compared with the sum (3.0) of the three link lengths the usable workspace of the mechanism is very small. And Figs. 18 and 19 can present an insight on the MIC, which show that the MIC radius is also small. Especially, from Fig. 19 or Eq. (36), the MIC radius can be obtained as

$r_{MIC} = 0.1875$. Then, the MIC radius R_{MIC} of the dimensional mechanism is $R_{MIC} = 32r_{MIC} = 6.0$ mm. All in all, the results shown in Figs. 11, 13, 17–19 can provide enough information for him to reach such a result that the usable workspace of the mechanism is comparative very small. He can even know the general workspace shape of the mechanism.

12. Conclusions

In this paper, the singularity and workspace for the 5R symmetrical parallel mechanism are investigated systematically in an established design space made up of two independent non-dimensional parameters. The analysis shows that

- Every mechanism has the stationary singularity, where at least one leg reaches its limit;
- The analysis on the theoretical workspace cannot give us enough information on the workspace performance of the 5R parallel mechanism. Based on this analysis, one cannot design such a mechanism with respect to the workspace performance;
- The mechanisms in the sub-region IIIa where $r_1 < r_3$ and $r_1 + r_3 < r_2$ in the established design space do not have the uncertainty singularity, which usually occurs inside the workspace. The workspace of such a mechanism is non-continuous and normally not large;
- For the mechanisms in the sub-region IVa where $r_1 + r_3 < r_2$ and $r_1 > r_3$, there is no singularity that B_1PB_2 is completely extended in their workspaces;
- The mechanisms in other sub-regions where $r_1 + r_3 > r_2$ have the singularity that B_1PB_2 is completely extended;
- The mechanism in any one of the sub-regions IVa, IVb, Va and Vb, where $r_1 > r_3$ and $r_2 > r_3$, can have two actuated crank links if the "+ −" working mode is adopted;
- The usable workspace presented in Fig. 17 is such a workspace that the mechanism with the "+ −" working mode can reach continuously without singularity;
- The MIW which is characterized by the MIC defined in this paper cannot stands for the exact area of the usable workspace. But, with the help of the workspace shape distribution characteristics, the MIC radius atlas can give us enough information that which mechanism can have a large usable workspace and which one cannot. Our objective is to give a comparative result. The MIC radius atlas is sure to do this. The MIW can be used to evaluate other performances, which are defined with respect to a workspace;
- In the design space with non-dimensional parameters, the 5R parallel mechanism with the parameters $r_1 = 1.5$, $r_2 = 1.5$ and $r_3 = 0.0$ has the maximum usable workspace and MIW. The second kind of singular locus of the mechanism is only one point when B_1PB_2 is completely extended, and is the complete workspace when the points B_1 and B_2 are coincident. A mechanism with the neighboring parameters in the design space also has a relative large workspace and MIW;
- The MIC radius R_{MIC} of a dimensional 5R parallel mechanism is D times the MIC radius r_{MIC} of the corresponding non-dimensional mechanism. This means that the MIW of a dimensional mechanism is D^2 times the MIW of the corresponding non-dimensional mechanism, and so is the usable workspace;

- Based on the results shown in Figs. 11, 13, 17, 18 and 19, one can know the singularity and workspace performances of a 5R parallel mechanism with any possible geometric parameters R_1, R_2 and R_3;
- The singularity, usable workspace, MIC and MIW results presented here will be different for the mechanism with other working modes except the "+ −" mode.

The results of the paper are very useful for the optimum design of the mechanism.

Acknowledgement

The first author wishes to acknowledge the support from the Alexander von Humboldt (AvH) Foundation when he was the AvH Research Fellow at University of Stuttgart in Germany.

References

[1] K.M. Lee, D.K. Shah, Part 1: kinematic analysis of a 3-DOF in-parallel actuated manipulator, IEEE J. Robotic. Auotm. 4 (1988) 354–360.
[2] J.-P. Merlet, Direct kinematic and assembly motion parallel manipulators, Int. J. Robotic. Res. 11 (2) (1992) 150–162.
[3] J.P. Merlet, C.M. Gosselin, N. Mouly, Workspace of planar parallel manipulators, Mech. Mach. Theory 33 (1/2) (1998) 7–20.
[4] C.M. Gosselin, J. Angeles, Singularity analysis of closed loop kinematic chains, IEEE Trans. Robotic. Autom. 6 (3) (1990) 281–290.
[5] X.-J. Liu, J. Wang, F. Gao, L.-P. Wang, On the analysis of a new spatial three degrees of freedom parallel manipulator, IEEE Trans. Robotic. Autom. 17 (6) (2001) 959–968.
[6] I.A. Bonev, D. Zlatanov, C.M. Gosselin, Singularity analysis of 3-DOF planar parallel mechanisms via screw theory, ASME J. Mech. Des. 125 (2003) 573–581.
[7] J.-P. Merlet, Designing a parallel manipulator for a specific workspace, The Int. J. Robotic. Res. 16 (1997) 545–556.
[8] E. Ottaviano, M. Ceccarelli, Optimal design of CaPaMan (Cassino Parallel Manipulator) with a specified orientation workspace, Robotica 20 (2002) 159–166.
[9] C.M. Gosselin, J. Angeles, The optimum kinematic design of a spherical three degree-of-freedom parallel manipulator, J. Mech. Trans. Autom. Des. 111 (1989) 202–207.
[10] C.M. Gosselin, The optimum design of robotic manipulators using dexterity indices, Robotic. Auton. Syst. 9 (1992) 213–226.
[11] R.S. Stoughton, T. Arai, A modified Stewart platform manipulator with improved dexterity, IEEE Trans. Robotic. Autom. 9 (2) (1993) 166–173.
[12] J. Ryu, J. Cha, Optimal architecture design of parallel manipulators for best accuracy, in: Proceedings of the 2001 IEEE/RSJ International Conference on Intelligent Robots and Systems, Maui, Hawwaii, USA, 2001, pp. 1281–1286.
[13] H.S. Kim, L.-W. Tsai, Design optimization of a Cartesian parallel manipulator, J. Mech. Des. 125 (1) (2003) 43–51.
[14] G. Alıcı, An inverse position analysis of five-bar planar parallel manipulators, Robotica 20 (2002) 195–201.
[15] F. Gao, X. Zhang, Y. Zhao, H. Wang, A physical model of the solution space and the atlases of the reachable workspaces for 2-DOF parallel plane wrists, Mech. Mach. Theory 31 (2) (1996) 173–184.
[16] J.J. Cervantes-Sánchez, J.C. Hernández-Rodríguez, J.G. Rendón-Sánchez, On the workspace, assembly configurations and singularity curves of the RRRRR-type planar manipulator, Mech. Mach. Theory 35 (2000) 1117–1139.

[17] F. Gao, X.-J. Liu, W.A. Gruver, Performance evaluation of two-degree-of-freedom planar parallel robots, Mech. Mach. Theory 33 (6) (1998) 661–668.
[18] F.C. Park, J.W. Kim, Singularity analysis of closed kinematic chains, J. Mech. Des. 121 (1999) 32–38.
[19] J.J. Cervantes-Sánchez, J.C. Hernández-Rodríguez, J. Angeles, On the kinematic design of the 5R planar, symmetric manipulator, Mech. Mach. Theory 36 (2001) 1301–1313.
[20] X.-J. Liu, The relationships between the performance criteria and link lengths of the parallel manipulators and their design theory, PhD Thesis, Yanshan University, Qinhuangdao, China, 1999.
[21] G. Alıcı, B. Shirinzadeh, Optimum synthesis of planar parallel manipulators based on kinematic isotropy and force balancing, Robotica 22 (2004) 97–108.
[22] X.-J. Liu, J. Wang, G. Pritschow, Performance atlases and optimum design of planar 5R symmetrical parallel mechanisms, Mech. Mach. Theory, Paper No. MMT39-168, submitted for publication.
[23] I.A. Bonev, C.M. Gosselin, Singularity loci of planar parallel manipulators with revolute joints, in: 2nd Workshop on Computational Kinematics, Seoul, South Korea, May 20–22, 2001.